Regimes with Sharp Density Profile and Enhanced Energy Confinement under Deuterium Pellet Injection and ECRH in T-10

Yu.D.Pavlov, Yu.N.Dnestrovskij, A.A.Borshegovskij, V.V.Chistiakov, A.V.Gorshkov, Yu.V.Gott, N.V.Ivanov, A.M.Kakurin, L.N.Khimchenko, A.V.Khramenkov, N.A.Kirneva, S.V.Krylov, V.A.Krupin, V.V.Matveev, T.B.Mialton, A.Yu.Novikov, V.V.Piterskij, S.V.Popovichev, V.V.Prut, I.N.Roy, M.B.Safonova, V.V.Sannikov, S.A.Shibaev, A.V.Sushkov, V.M.Trukhin, V.A.Volkov, V.S.Zaveriaev.

Nuclear Fusion Institute, Russian Research Center "Kurchatov Institute", Moscow, Russia

e-mail contact of main author: pavlov@nfi.kiae.ru

Abstract. Experiments with deuterium pellet injection have been carried out on T-10. The main plasma parameters are as follows: $I_p \approx 250$ - 300 kA, $n_e \approx (3 - 4)\times10^{13}$ cm^{-3}, $P_{ECRH} \approx 400$ - 700 kW. A deuterium pellet was injected into the plasma at the stage of auxiliary ECRH. The main results are as follows: (a) a rapid sharpening of the plasma density profile with the increase of $n_e(0)$ after pellet injection and the sustainment of this profile during the whole ECRH pulse while the averaged chord density remained constant; (b) the lowering of $Z_{eff}(0)$ and the redistribution of $Z_{eff}(r)$; (c) the growth of ion temperature ; (d) the increase of plasma energy content and of energy confinement time τ_E by a factor of ~ 1.5 as compared to τ_E before pellet injection. The experimental results obtained are close to the RI-mode in TEXTOR after impurity feeding and can be described by the Canonical Profiles Transport Model.

Experiments with deuterium pellet injection have been carried out on T-10. The scenario of such experiments is illustrated by Fig. 1. The additional ECRH pulse was started on the steady-state phase of the plasma discharge. The duration of the gyrotron pulse was up to 400ms. A deuterium pellet was injected at 50 - 100 ms after the start of the gyrotron pulse. The main plasma parameters are as follows: $I_p \approx 220$ - 300 kA, $n_e \approx (3 - 4)^x10^{13}$ cm^{-3}, $P_{ECRH} \approx$ 400 - 700 kW. In the following we will discuss the regimes with $I_p \approx 300$ kA, $n_e \approx 3^x10^{13}$ cm^{-3}, $P_{ECRH} \approx 550$ kW. The location of the most intensive pellet ablation was approximately at 0.7a, where "a" is the minor plasma radius.

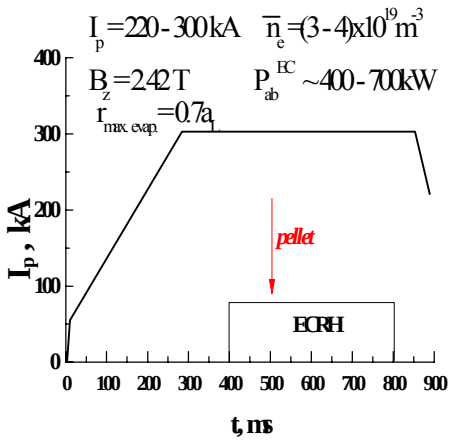

Fig. 1 Scenario of experiments.

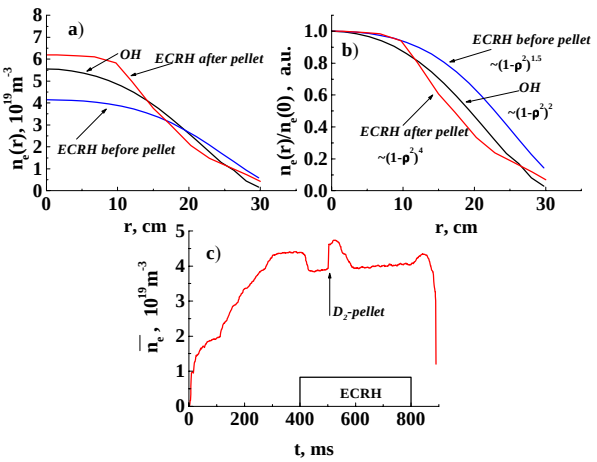

Fig. 2. Evolution of density profile (a,b) and averaged chord density (c) during a pulse with D_2 pellet injection.

Deuterium pellet injection during ECRH leads to essential changes of almost all the plasma parameters. The density profile after pellet injection becomes "tablelike" in form with a sharper gradient (Figs. 2(a,b)). This sharp profile exists during the whole ECRH pulse with a practically unchanged averaged density value (Fig. 2(c)). Such a density behaviour is specific to the stage of additional ECR heating only. If the deuterium pellet was injected into the plasma at the OH stage the density profile, after first being sharpened by pellet injection, was restored to its initial shape. The time of the profile restoration is close to the time for the average density to return to the initial value, i.e. it is essentially less than the duration of the ECRH pulse. It should be noted that in the OH regimes all plasma parameters are restored to their initial values in the same time. The behaviour of the plasma parameters for the OH stage disagrees with the experimental results from the Tuman-3 tokamak [1], so only the regimes with pellet injection during the ECRH pulse are presented below. The electron temperature T_e and the intensity of the SXR emission drop very quickly after pellet injection (step a time less than 100 μs) and then increase slowly up to a new stationary value (Figs. 3(a), 4(a)). Such a behaviour of the electron temperature and the SXR emission was observed practically simultaneously for all plasma radii. Figures 3(b), 4(b) show a temporal evolution of the electron temperature and SXR emission profiles for several times marked on Figs. 3(a), 4(a). The normalized profiles of $T_e(r)$ are slightly broader after pellet injection than before pellet injection (Fig. 3(c)).

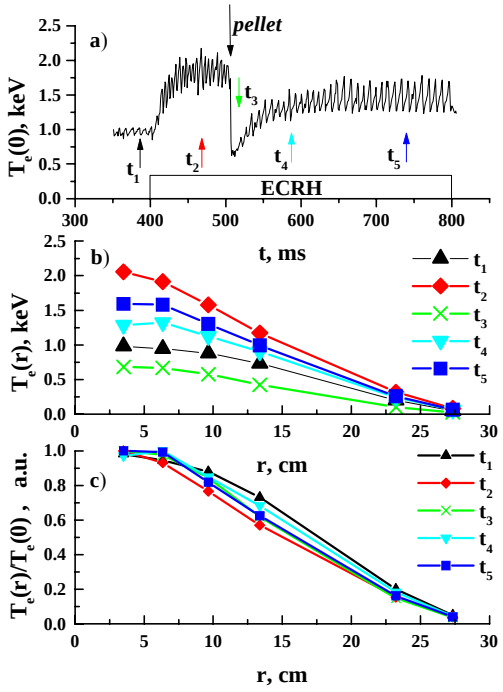

Fig. 3. Behaviour of the central electron temperature in time (a) and corresponding electron temperature profiles (b,c).

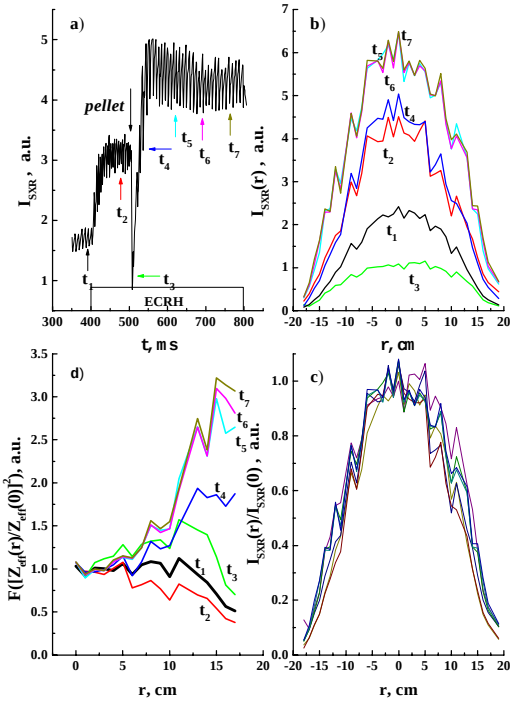

Fig. 4. Behaviour of SXR emission in time (a) and corresponding SXR emission profiles (b,c). Estimated radial $F([Z_{eff}(r)/Z_{eff}(0)]^2)$ distributions (d).

The chord intensity profiles of SXR normalized to the central values (Fig. 4c) were remained almost the same or were slightly broader after pellet injection than before pellet injection. At the same time (as one can see from Fig. 2) the electron density profile was sharpened greatly during the increase of the core density. One can calculate the ratio of normalized intensities of SXR and square normalized densities. This function

$F([Z_{eff}(r)/Z_{eff}(0)]^2)$ reflects mainly the radial distribution of square Z_{eff} (r). The temporal behaviour of this function shown in Fig. 4(d). One can see that the profiles of this function change from relatively flat ones in the core and slightly tapered ones on the periphery before the pellet injection (times t_1 and t_2) to steep ones at the edge of the plasma after pellet injection. This means that the Z_{eff} profile becomes hollow in the plasma centre and this distribution is kept during the ECR pulse. The estimated profiles of $Z_{eff}(r)$ are shown in Fig. 5(a). These Z_{eff} profiles were obtained from the visible optical continuum measurements. One can see that the value of $Z_{eff}(0)$ decreases after D_2 pellet injection. Figure 5(b) shows the temporal behaviour of the plasma parameter $\overline{Z}_{eff}$ derived from the visible optical continuum measurements for the described regime and for the regime without pellet injection. One can see that just after the pellet injection the value of $\overline{Z}_{eff}$ drops sharply afterward grows to its previous value. It should be noted that there are many shots in which $\overline{Z}_{eff}$ dropped more significantly after pellet injection and then subsequently increased but did not achieve the value typical for regimes without pellet injection.

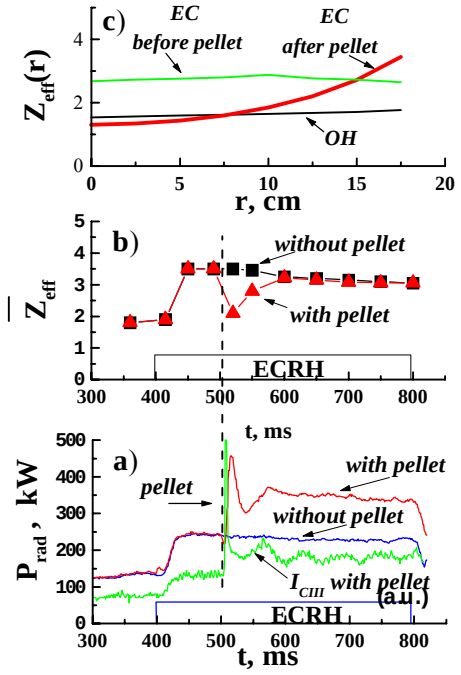

Fig. 5.(a) Radial distribution of Z_{eff} ; (b) temporal behaviour of $\overline{Z}_{eff}$; (c) behaviour of radiation losses and CIII line intensity emission.

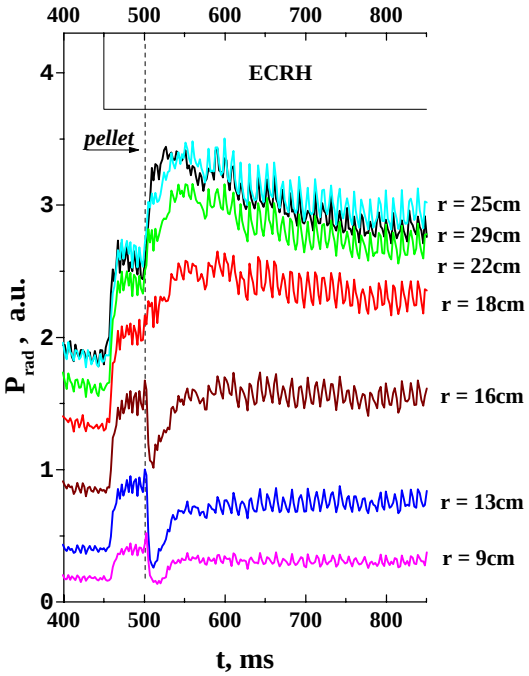

Fig. 6. Behaviour of radiation losses for different chords.

.

The re-formation of the Z_{eff} profile is confirmed by radiation loss signals for the different chords (Fig. 6). One can see that the signals from the central chords decrease and those from the peripheral chords increase after pellet injection, in contrast to the density profile behaviour. It is likely that such behaviour of radiation losses is connected with a displacement of impurities from the plasma core to the periphery. It is in agreement with the temporal behaviour of the Z_{eff} profile. The total value of radiation losses increases from 30% to 40% of the deposited power. This increase is connected with the increase of the radiation losses on the periphery, which is in agreement with the increase of the CIII line intensity emission (Fig. 5(c)).

The pellet injection causes both the broadening of the ion temperature profile and the increase of the $T_i(0)$ value (Fig. 7(b)). These were measured by the chargeexchange diagnostic and were calculated from the absolute value of the neutron yield (Fig. 7(a)). The neutron yield increases by up to a factor of 10 in the case shown. The evaluation of the ion energy confinement time τ_{Ei} has shown that in the case of pellet injection τ_{Ei} increases byup to a factor 2 (Fig. 7(c)). The pellet injection causes the change of values of β, stored energy W and global energy confinement time τ_E. Figure 8 demonstrates the temporal behaviour of these plasma parameters for discharges with and without pellet injection. One can see the increase of these values by up to ~ 1.6 times during pellet injection. The global energy confinement time for the regime with $P_{ab}^{EC} \sim 620$ kW reverts to the level of the OH energy confinement time. Also, it is necessary to note that the plasma stored energy increases by about 3 times due to pellet injection in comparison with the increase due to additional ECRH only.

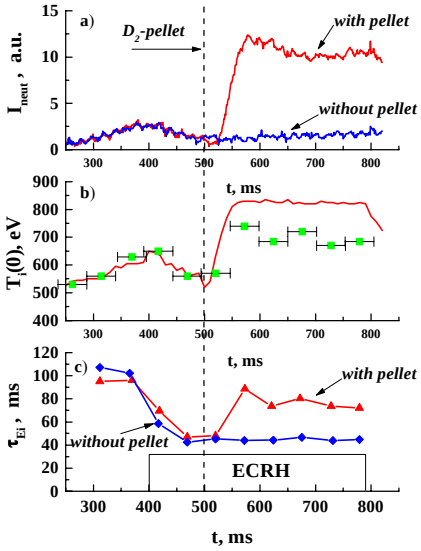

Fig. 7. (a) Temporal behaviour of the neutron yield; (b) the central ion temperature $T_i(0)$ (points are from the charge-exchange diagnostic, line is from the neutron yield); (c) ion energy confinement time τ_{Ei}.

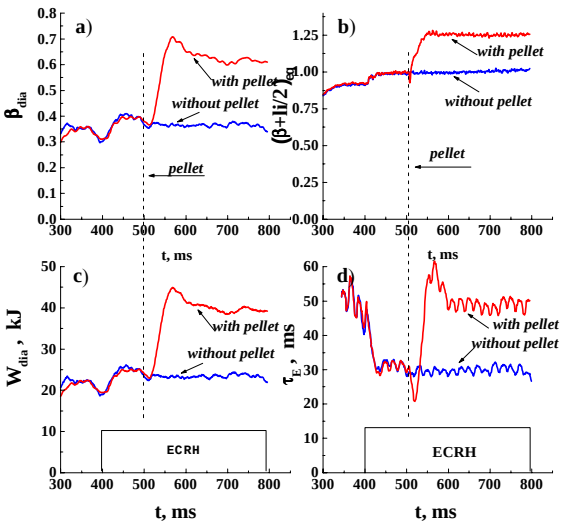

Fig. 8. Temporal evolution (a) value of β_{dia}; (b) the value of $(\beta+l_i/2)_{eq}$; (c) stored energy W; (d) global energy confinement time τ_E.

It is likely that such changes of the global plasma parameters are connected with the re-formation of the density profile and the Z_{eff} profile after pellet injection. The new distribution of plasma parameters is similar to the events in TEXTOR, which is described by the Canonical Profiles Transport Model [2]. According to this model, the transition from L to RI-mode occurs at the appearance of the hollow profile of Z_{eff}. Apparently a similar situation is realized in the T-10 Pellet Enhanced Confinement regime (PEC) with pellet injection described above. The calculations which were carried out by this transport model have shown a good agreement with experimental data.

Resume

1. Deuterium pellet injection during ECRH leads to essential changes of almost all the plasma parameters.
2. The plasma density profile changes radically and becomes "tablelike" in shape, with steep gradients inside the region $0.4<r/a<0.6$. This shape is conserved up to the end of the gyrotron pulse.

3. The electron temperature and SXR intensity profiles show little changes.
4. The $Z_{eff}(r)$ profile changes from flat to hollow due to the displacement of impurities from the plasma core to the edge with the decrease of the central value.
5. The ion temperature profile broadens and its absolute value $T_i(0)$ increases by a factor of 1.3.
6. The neutron emission increases by a factor of up to 10.
7. The ion energy confinement time increases by a factor of 2.
8. The energy storage increases by a factor of up to 1.6.
9. The global energy confinement time for the regime with $P_{ab}^{EC} \sim 620$ kW increases by a factor of 1.6 also, returning to the OH energy confinement time.
10. Such changes of global plasma parameters during the PEC regime can be described by the Canonical Profiles Transport Model modified for the RI-mode.

References

[1] Askinazi L.G., Golant V.E., Lebedev S.V., et al., " H-mode in the TUMAN-3 tokamak triggered by edge plasma perturbations", Phys. Fluids B, v.5 (1993), pp.2420-2427.

[2] Dnestrovskij Yu.N., "Simulation of RI mode in TEXTOR by the Canonical Profiles Transport Model", 26th EPS Conference on Controlled Fusion and Plasma Physics, Maastricht, ECA, v.23J (1999), p.817.

This work is supported by the Ministry of Atomic Energy of the Russian Federation (contract No. 69F) and the Ministry of Science of the Russian Federation (Federal Programme "Controlled Fusion and Plasma Processes").